Physica Medica 67 (2019) 100–106

Contents lists available at ScienceDirect

Physica Medica

journal homepage: www.elsevier.com/locate/ejmp

Original paper

Computed tomography-based virtual simulation versus ultrasound-based clinical setup in electron breast boost radiotherapy: Methodology for CT-based electron virtual simulation

Monica Serban[a,*], Christine Lambert[b], Russell Ruo[a], Ciro Maietta[b], William Parker[a], Michael Evans[a], Tarek Hijal[b]

[a] Department of Medical Physics, Cedars Cancer Centre, McGill University Health Centre, Glen Campus, 1001 Décarie Boul., Montreal H4A 3J1, Canada
[b] Department of Radiation Oncology, Cedars Cancer Centre, McGill University Health Centre, Glen Campus, 1001 Décarie Boul., Montreal H4A 3J1, Canada

ARTICLE INFO

Keywords:
Electron breast boost
Electron clinical setup
Ultrasound target delineation
CT target delineation
En-face electron field
CT virtual simulation

ABSTRACT

Purpose: To compare clinical setup using ultrasound (U/S)-delineated target versus computed tomography (CT) virtual simulation using CT-outlined target in breast electron boost. To describe a methodology for electron virtual simulation and collision testing with the treatment planning system (TPS).
Methods: The two techniques were compared in a prospective study on 12 patients, who were treated using a clinical setup. Target definition was performed by both U/S and CT imaging. The U/S-based target was made visible on CT images by placing a radio-opaque wire on U/S skin markings. The dose distribution of the clinical setup was reproduced in the TPS using the actual electron patient treatment parameters. A CT-based TPS virtual simulation/dose optimization was compared to the clinical setup technique.
Results: Mean beam aperture was larger by 16.3 cm^2 ($p = 0.011$) for U/S compared to CT-outlined target. Target mean depth difference (CT minus U/S) was 0.03 cm ($p = 0.875$). Target coverage at depth was adequate in all cases with CT-based simulation while under/overcovering the target at depth by more than 5 mm in 2 out of 12 cases with clinical setup. Mean target $V_{90\%}$ was 98.5% (CT-based simulation) and 84.4% (clinical setup). Ipsilateral lung/breast were better spared with CT-based simulation. To date, the methodology for CT virtual simulation was applied on 152 patients and collision was avoided in all cases.
Conclusions: CT-based simulation and target delineation allows for improved definition of the en-face electron field with less amount of normal tissue irradiated while including the entire target with an adequate margin and optimal electron energy.

1. Introduction

Whole breast irradiation, delivered typically via tangential fields, is an important part of breast conserving cancer therapy [1–3]. Several studies have indicated that an additional boost to the tumour bed reduces the risk of local recurrence [4–9].

Different techniques have been used to deliver the dose to the tumour bed, such as brachytherapy interstitial implants, photon irradiation, intraoperative radiotherapy or electron irradiation. A commonly used technique for breast boost is the en-face electron field. The electron field is relatively easy to plan and set up, and is the preferred technique for superficial tumours (with maximum depth less than 4 cm). Determining the electron beam aperture is crucial for this technique and relies on the method used for lumpectomy localization. The ideal method to define the surgical cavity for electron boost is unclear [10,11]. Palpation and scar-based planning have been shown to be inferior to CT and MRI localization techniques [12–18]. Significant differences in center and extent of the tumour bed when comparing the surgical clips to CT has been demonstrated: an underestimation of the size of the tumour bed, as defined by the clips, justified the integration of CT information in boost planning [19]. Very few studies exist regarding ultrasound (U/S) based planning. Comparison of diagnostic U/S to surgical clips for lumpectomy localization [11] demonstrated that 65% of the U/S localizations were adequate (surgical clips covered by 90% isodose line), 28% were marginal (any surgical clip lying between 80% and 90% isodose line) and 7% were inadequate (any surgical clip would not be encompassed by 80% isodose line). In addition, 3D U/S imaging for interfraction tumour bed motion demonstrated an average

* Corresponding author.
E-mail address: monica.serban@mcgill.ca (M. Serban).

https://doi.org/10.1016/j.ejmp.2019.10.030
Received 12 June 2019; Received in revised form 6 October 2019; Accepted 15 October 2019
Available online 06 November 2019

center-of-mass displacement of approximately 4 mm between U/S and CT [20].

Previously at our institution, treatment planning for electron boost was performed by clinical setup of the en-face electron field at the treatment unit, based on U/S evaluation of the tumour bed extension and depth. With time, when a commercially treatment planning system (TPS) with an electron Monte Carlo (eMC) dose calculation algorithm became available, the electron breast boost technique transitioned towards CT-based target delineation, virtual simulation and dose optimization. Multiple studies document the dosimetric accuracy of electron Monte Carlo technique for treatment planning dose calculation [21,22] but these studies do not address the clinical process of virtual simulation using image-based treatment planning. In addition, a few clinical studies compare visualization of breast tumour bed using U/S versus CT [20,23], while the dosimetric impact between U/S versus surgical clips approaches has been quantitatively described in one recent study [24]. The authors concluded that, on average, 17% of the surgical clips-based target volume was covered by 90% of the prescribed dose, when the electron field was defined on the U/S-based target volume. The present work presents (1) a prospective study of twelve patients comparing the dosimetric differences between CT-based tumour bed delineation and virtual simulation versus the U/S-based clinical setup technique and (2) a methodology for simulation of breast electron boost using CT-based virtual simulation and target delineation.

2. Materials

2.1. CT-based virtual simulation versus U/S-based clinical setup for electron breast boost

A prospective study that compared our conventional technique, consisting of a clinically setup electron field based on 2D U/S target delineation, to the CT-based virtual simulation of the en-face electron field and CT-delineated target was conducted. A total of twelve patients who underwent breast-conserving surgery, whole breast irradiation and were deemed in need of receiving an electron boost to the surgical cavity were enrolled in this study. Approval to conduct the study was given by the institutional ethics review board. Eight patients out of twelve received cytotoxic chemotherapy between the surgery and radiotherapy. For all twelve patients, the prescribed dose to the boost PTV was 10 Gy in 4 fractions.

In general, radiotherapy started 4 weeks after completion of adjuvant chemotherapy, or within no more than 9 weeks after definitive surgery, if chemotherapy was not given. The tumour bed became more difficult to identify as time passed, due to absorption of the seroma and healing of the site. All delineated tumour beds were evaluated and scored using the following cavity visualization score (CVS) (20): 1, cavity not visualized; 2, cavity visualized but margins indistinct; 3, cavity visualized with some distinct margins; 4, cavity visualized with all but one margin distinct; and 5, all cavity margins clearly defined.

On the day of the electron boost simulation the patients underwent 2D U/S and skin marking in the radiology department. The depth from the skin surface to the deepest part of the surgical cavity was measured by 2D U/S.

Following the U/S simulation, an additional planning CT was acquired for the study. The patients were placed in the supine position and immobilized in a Vac-Lok™ (CIVCO Medical Solutions) with both arms up in the overhead position. A radiation oncologist defined the U/S target volume (U/S TV) by adding a 1–1.5 cm margin around the U/S skin markings. Radio-opaque wire was carefully placed along the U/S TV, as well as along the scar.

The patients were treated using our conventional technique where the electron field parameters (gantry, collimator and couch angle) were determined during a clinical setup at the treatment unit. The electron energy was selected such that the target depth (as per U/S) was within the 90% isodose line. The monitor units (MUs) were calculated using the prescribed dose (to typically 90% isodose) and output measurements for the treatment cutout size and selected electron energy.

For our dosimetric study, two separate breast boost plans were produced for each patient. First, a plan, using the CT images and the radio-opaque wire as a surrogate for the U/S TV, was generated to mimick the clinical setup treatment plan. The actual treatment parameters (gantry, collimator, couch, energy and number of MUs) were used in the TPS to reproduce the dose delivered to the patient. The electron field aperture in the TPS was determined from the radio-opaque wire used at the time of CT to mark the U/S TV. Second, a hypothetical plan, using CT-based virtual simulation and CT target delineation, was produced as per the methodology described below (Materials and Methods, Section 2).

To determine which of the two techniques was superior in terms of electron energy selection, we studied the correlation between the maximum depth of the planning target volume (PTV) as delineated on CT with the depth of the 9.5 Gy (95% of prescription) isodose line corresponding to the two techniques, where the depth of the 9.5 Gy isodose was used as a surrogate for selected electron energy with each technique. The depths of the 9.5 Gy isodose lines were measured in both plans and plotted as a function of the CT-based PTV maximum depth, whereby CT was considered as the gold standard for target depth definition. The best energy – target depth correlation would consist of points lying on the identity line.

Dose volume histograms (DVHs) were used to evaluate target and organs at risk (OARs) doses. The analysis included the percentages of the PTV volume encompassed by the 95%, 90%, 80% and 50% isodose volumes. Doses to the ipsilateral lung and ipsilateral breast minus PTV were compared between the two techniques.

2.2. Methodology for CT-based virtual simulation of electron breast boost

The following describes the methodology developed in our clinic for CT-based virtual simulation for breast boost electron therapy.

2.2.1. Acquisition of planning CT data

Each patient is positioned supine on a 10–15° inclined breast board (CIVCO Medical Solutions) with both arms elevated above the head in an arm support and their legs resting on a knee sponge. A planning CT is obtained with 3 mm slice thickness. Typically, the same planning CT scan is used for both, the whole breast irradiation and the tumour bed electron boost treatment plans. A radio-opaque wire is carefully placed along the scar to indicate its location on the CT images and for in-room patient setup purposes.

2.2.2. CT target delineation

The tumour bed is delineated according to the visualized tumour bed, and surgical clips when available. The clinical target volume (CTV) is defined by adding an isotropic margin of 5 mm to the cavity and trimmed from the pectoralis muscle. An additional 5 mm margin is added isotropically from the edge of the CTV to define the planning target volume (PTV). The PTV is trimmed such that the margin at depth (distal) amounts for 2 mm from the CTV edge.

2.2.3. CT-based virtual simulation of electron treatment field and collision detection

The electron breast boost treatments is planned using the treatment planning system (TPS) and eMC dose calculation algorithm. The beam orientation and couch position is based on the external body and target contour so as to create an en-face beam. The gantry angle, followed by the couch angle, are adjusted such that the electron field is as perpendicular as possible to the outer body contour (skin surface), as shown in Figs. 1 and 2. To visualize the target in the beam's eye view (BEV), the patient is first rotated by the couch angle in the coronal view (Fig. 1b) and subsequently rotated by the gantry angle in the axial view (Fig. 1a).

The electron field borders are defined based on the PTV contour

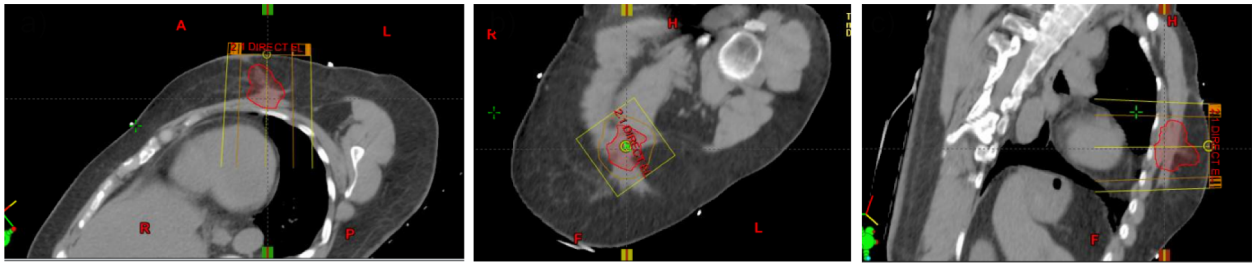

Fig. 1. Three orthogonal cross-sections of an en-face electron beam with 45° gantry angle and 30° couch rotation as viewed from the BEV's perspective: a) para-transverse, b) para-coronal, c) para-sagittal. Panels a and c show electron beam axis optimized to be as perpendicular as possible on patient body surface.

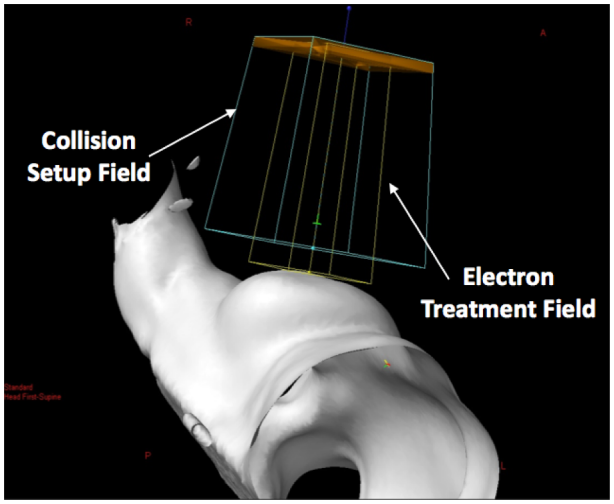

Fig. 2. Detection of potential collision between electron applicator and patient using Eclipse TPS: electron treatment field at 100 cm SSD (yellow); collision setup field at 102.5 cm SSD (blue) showing applicator outer edges. Absence of contact between the edges of the simulated collision field and patient skin surface indicated no collision. (For interpretation of the references to colour in this figure legend, the reader is referred to the web version of this article.)

projection on the BEV plus an isotropic margin of 0.8 cm to account for the electron beam penumbra. The electron energy and the isodose line used for dose prescription are chosen such that 90% of the prescribed dose covers more than 95% of the PTV ($V_{90\%} > 95\%$), and a maximum dose allowed of approximately 110% ($D_{max} \sim 110\%$) of the prescribed dose. The normalization point is set at the depth of maximum dose on electron beam's central axis.

To detect a possible collision between electron applicator and patient, a setup field, mimicking the outer dimensions and the relative position of the applicator with respect to patient skin is created (Fig. 2). When using Eclipse™ (Varian Medical Systems, Palo Alto, California, USA) as TPS, the base of the radiation field is always displayed at the level of the isocentre (100 cm SSD), in the 3D visualization window. The collision setup field is planned with identical field parameters as those of the electron treatment field except for the: (1) jaw settings, which are set to the outer dimension of the applicator bumper, and (2) SSD, which is increased by 2.5 cm as to account for the air gap between the actual electron applicator outer edge (bumper) and patient skin.

2.3. Statistical analysis

Data was analyzed as a paired sample based on the Student's *t*-test using the STATA statistical software (v15.1, College Station/TX/USA). The assumptions were checked by plotting the differences against the averages (Bland-Altman plot) and by Q-Q plots of the differences. Estimates were given with 95% confidence intervals.

3. Results

3.1. CT-based virtual simulation versus U/S-based clinical setup for electron breast boost

The median time interval between surgery and electron boost treatment was 25 weeks (range 10–38 weeks). For our study, the post-operative cavity was graded "highly visible" in one third (CVS 4 and 5) and "visible" in two thirds of the cases (CVS 3). Patient and treatment characteristics for the twelve patients are presented in Table 1, with each patient identified by a number and a colour corresponding to the colour scheme of Fig. 7.

Table 1
Treatment characteristics for the twelve patients including U/S and CT-based aperture areas, tumour bed depths, PTV V_{9Gy} and CT-based PTV volumes. The averages are indicated with 1 standard deviation (SD). Each patient was assigned a number and colour according to the colour scheme used in Fig. 7.

Patient No. (Colour)	U/S Aperture Area (cm^2)	U/S Depth (cm)	CT Aperture Area (cm^2)	CT Depth (cm)	CT Target Vol. (cm^3)	U/S PTV V_{9Gy} (%)	CT PTV V_{9Gy} (%)
1 (bue)	97	3.0	32	2.3	30.4	85.0	97.3
2 (violet)	59	3.3	48	2.7	52.6	81.9	97.3
3 (black)	47	3.0	40	2.4	42.6	96.2	100.0
4 (yellow)	66	2.6	43	4.0	59.7	98.6	98.1
5 (cyan)	66	2.2	29	3.5	21.0	67.1	98.6
6 (maroon))	36	1.0	28	0.9	16.6	81.4	97.4
7 (red)	57	4.0	49	3.3	80.8	95.9	98.4
8 (brown)	49	2.3	30	2.9	19.9	70.8	98.5
9 (magenta)	57	1.9	60	2.0	51.8	86.5	98.0
10 (turquoise)	46	2.3	31	2.2	36.0	94.2	99.1
11 (green)	42	4.7	36	4.5	49.0	99.9	100.0
12 (orange)	37*	3.0	37*	3.1	46.9	54.7	99.9
Average (1 SD)	54.8 (16.6)	2.8 (1.0)	38.5 (9.8)	2.8 (1.0)	42.3 (18.7)	84.4 (14.1)	98.5 (1.0)

*Although the areas of the U/S and CT apertures were identical for Patient 12, their shape and center-of-mass were different, resulting in contrasting target coverages with the two methods.

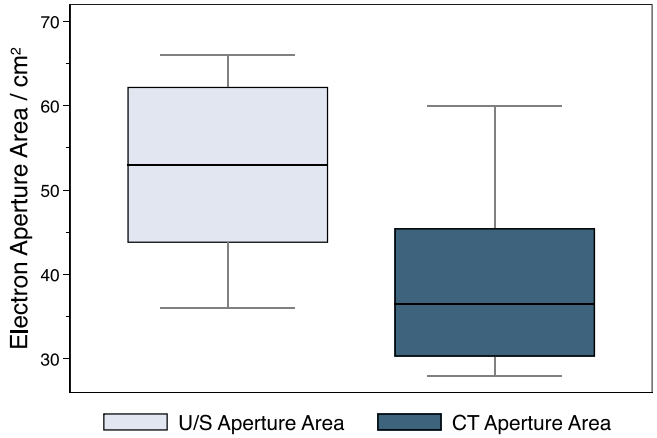

Fig. 3. Electron aperture areas based on U/S (light blue) and CT (dark blue) imaging modalities. The box displays the interquartile range, (IQR: 25th to 75th percentiles), and the median. The whiskers display the upper and lower values within 1.5*IQR beyond the 25th and 75th percentile. (For interpretation of the references to colour in this figure legend, the reader is referred to the web version of this article.)

3.1.1. Electron aperture areas

The electron beam aperture surface, as projected on patient's skin, was significantly larger for U/S as compared to CT, with a mean of 54.8 cm^2 and 38.5 cm^2, respectively (Table 1 and Fig. 3). Mean aperture area was by 16.3 cm^2 (95% CI [4.8; 28.1]) larger for U/S than for CT ($p = 0.011$).

Fig. 4a and c show the tumour bed and PTV contours on two different axial slices (positions of the CT slices are indicated by the black horizontal lines in Fig. 4b and d). Fig. 4b and 4d show BEVs of the electron field with the U/S-based clinical setup and CT-based virtual simulation. Field apertures were constructed to fit the U/S TV (demarcated by the radio-opaque wire, in blue) or to fit the CT-delineated PTV (in red) plus a 0.8 cm margin accounting for beam penumbra. It can be noted that for the case presented in Fig. 4, the clinically setup field aperture extends further cranially and caudally while being tighter on the medial lateral aspect of the breast when compared to the CT virtual simulation field aperture.

3.1.2. Tumour bed depth and choice of electron energy

Tumour bed depth differences as a function of the average tumour bed depths determined by the two methods (Table 1), mean difference, 95% CI (confidence interval) and 95% PI (prediction interval) are given in Fig. 5. The mean tumour bed depth difference (CT minus U/S) was 0.03 cm (95% CI [−0.42; 0.49]), ($p = 0.875$).

Fig. 6 shows the correlation between the depth of the 9.5 Gy isodose line and PTV maximum depth as a measure for appropriate electron energy selection. The solid line (unity line) indicates exact agreement between PTV maximum depth and 9.5 Gy isodose line depth. The two dashed lines delineate a band of ± 2 mm departure from identity. For the CT-based virtual simulation, the 9.5 Gy isodose line was, generally, more penetrating than the PTV maximum depth, by an average of 1.4 mm (range [−0.5; 3.1] mm). For the U/S-based clinical setup, the 9.5 Gy isodose depth was either more penetrating or shallower than the PTV maximum depth, deviating in two patients more than 5 mm from the unity line: average difference was 0.7 mm (range [−6.0; 6.1] mm).

3.1.3. DVH analysis

Fig. 7 shows PTV, breast-PTV and ipsilateral lung DVHs achieved with the two techniques. The mean PTV volumes (%) covered by 95%, 90%, 80% and 50% of the prescribed dose were 94.7%, 98.5%, 99.4% and 100%, respectively with the CT-based virtual simulation, and 69.7%, 84.4%, 90.3% and 96.3%, respectively with the U/S-based clinical setup. PTV $V_{9Gy,}$ given in Table 1, was improved by 14.1%

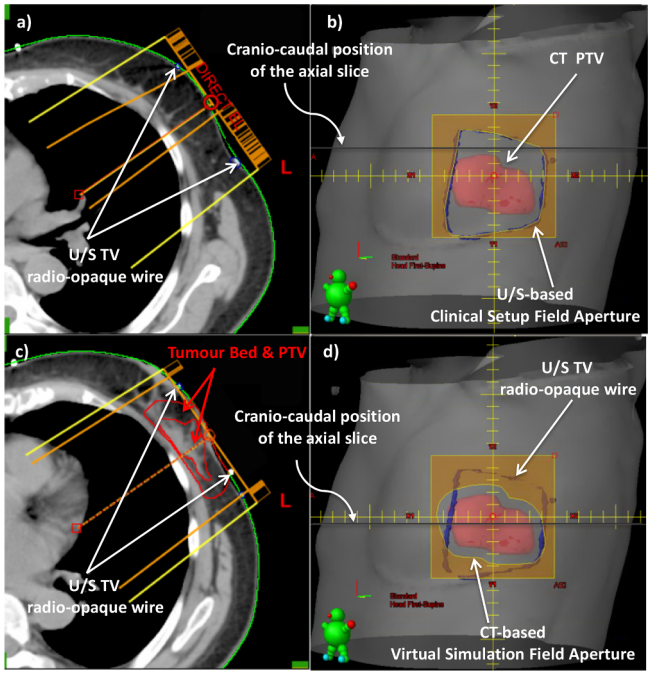

Fig. 4. a) and c) CT axial slices showing the tumour bed and PTV contours. b) BEV of the clinically setup electron field aperture demarcated by the radio-opaque wire in blue (includes the U/S defined tumour bed and an added margin for the electron field penumbra). The black horizontal line indicates the cranial-caudal level of the axial slice in panel a). d) BEV of the virtually simulated electron field based on the CT-delineated PTV plus an isotropic margin of 0.8 cm around the PTV accounting for the electron field penumbra. The black horizontal line indicates the cranial-caudal level of the axial slice in panel b). (For interpretation of the references to colour in this figure legend, the reader is referred to the web version of this article.)

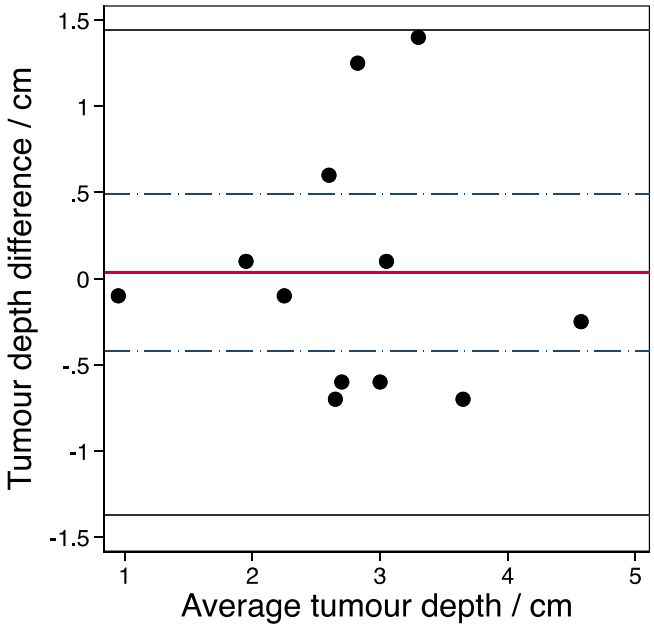

Fig. 5. Difference in tumour bed depth between CT and U/S imaging as a function of average CT and U/S tumour bed depths for the twelve patients. The mean tumour bed depth difference with the 95% CI (confidence interval) and 95% PI (prediction intervals) are displayed by thick red, dashed blue and thin black horizontal lines. (For interpretation of the references to colour in this figure legend, the reader is referred to the web version of this article.)

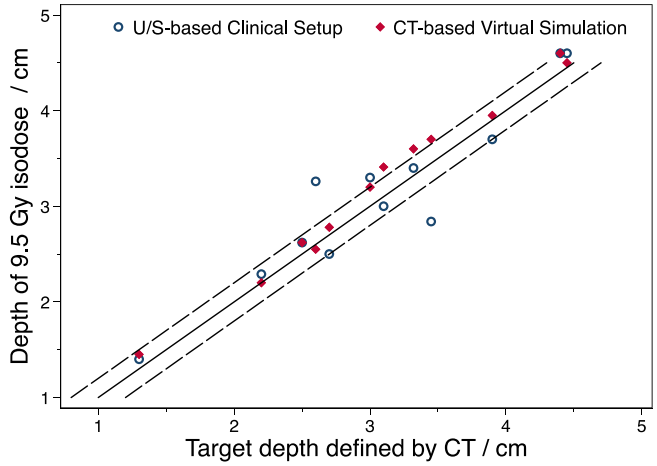

Fig. 6. Depth of the 9.5 Gy isodose line as a function of PTV maximum depth for U/S-based clinical setup and CT-based virtual simulation. The solid line indicates exact agreement between CT target depth and depth of the 9.5 Gy isodose line (unity line). The two dash-dotted lines delineate a band of ± 2 mm departure from identity.

(95%CI [5.2%; 23.2%]) for the CT-based virtual simulation (p = 0.005). Mean D_{max} to PTV was 11.1 (SD: 0.2) Gy and 11.1 (SD: 0.7) Gy for the CT-based and U/S-based techniques, respectively.

Due to the larger field apertures used with the clinical setup, the irradiated volumes to high and intermediate doses of ipsilateral breast tissue excluding PTV and to the ipsilateral lung were larger. Mean breast-PTV V_{9Gy} was by 4.9% (95%CI [0.9%; 8.9%]) larger with the clinical setup (12.1%) as compared to the CT-based virtual simulation (7.1%), (p = 0.020). Mean breast-PTV V_{5Gy} was by 7.1% (95%CI [0.9; 13.3]) larger for the clinical setup (20.3%) as compared to the CT-based virtual simulation (13.1%), (p = 0.028). Mean ipsilateral lung V_{1Gy} was by 3.3% (95%CI [−5.6; 12.3%]) larger for the clinical setup (27.2%) as compared to the CT-based virtual simulation (23.8%), however not statistically significant (p = 0.429).

3.2. Methodology for CT-based virtual simulation of electron breast boost

This study demonstrated that breast-boost virtual simulation of patients positioned on a breast board, with significant probability for collision, was feasible using the standard TPS and CT images of the patient. The key concept of the methodology was to create an auxiliary collision setup field that replicated the applicator outer dimensions and the distance relative to the patient. This auxiliary field and its relative position to patient's outer contour (3D skin rendering) could be visualized (Fig. 2) and therefore the potential of collision detected. Furthermore, the couch, gantry and collimator parameters for the en-face electron field was virtually simulated using the TPS 3D visualization tools and 2D orthogonal views (Figs. 1 and 2). This methodology helped in predicting potential collision and was proposed as a replacement of the clinically setup electron field based on U/S TV markings, with the patient in the treatment position at the treatment machine.

4. Discussion

In the past decade the CT-based simulation for electron breast boost treatments has been increasingly accepted in clinical practice. The present study quantified the dosimetric differences between the clinical setup of the electron field using U/S for target delineation and the CT-based virtual simulation. The second purpose of this study was to describe a methodology for electron virtual simulation and collision testing with a TPS.

Overall, the conventional simulation using U/S-based delineated target and clinical electron field setup at the treatment unit proved to be sub-optimal. Although larger breast areas, by on average 16.3 cm^2, were treated with the clinical setup method, they were not always suitably encompassing the CT-based defined PTV. This resulted in target coverage with the clinical setup method significantly inferior to the virtual simulation method, with PTV V_{9Gy} lower by 14.1% (p = 0.005) (84.4% clinical setup versus 98.5% CT virtual simulation). Sub-optimal target coverage as defined by surgical clips on CT when using U/S and clinical setup for patient treatment was previously reported by Aghili et al. [24]. However, the reported average $V_{90\%}$ was 16.7% as compared to 84.4% in our study. The discrepancy in findings with our study could be due to (1) large target volumes, of on average 95.2 cm^3, determined by clips delineation as compared to 42.3 cm^3 (Table 1) determined by seroma in our study; (2) greater target depths determined by clips in the Aghili et al. study, of on average 4.9 cm, which is consistently larger than their estimated tumour bed depths by U/S (by on average 3 cm).

Large discrepancies were found when comparing the CT to the U/S-defined field aperture in terms of both target center-of-mass position and dimensions. The larger electron apertures with the clinical setup method could be due to uncertainties in the scanning procedure and how the information from the U/S image of the outer edges of the tumour bed was translated to patient skin, resulting in an overestimation of the area to be treated.

Differences in target coverage at depth were dictated by target depths estimated from the respective imaging methods, added margins to account for CTV/setup errors and appropriate selection of the electron energy with the two techniques. The tumour bed depths were comparable between the two methods. However, the translation of target depth into appropriate electron energy selection was suboptimal in 2 out of 12 cases (17%) with the clinical setup method. The CT simulation resulted in an adequate target coverage at depth in all cases (Fig. 6). For the clinical setup, the 9.5 Gy isodose line was shallower than the PTV depth by ≥2 mm in 3 patients (Patients 2, 5 and 7), while in 1 out of the 3 patients (Patient 5) the PTV was undercovered by 6 mm (due to an underestimated U/S cavity depth by 1.3 cm compared to the surgical cavity on the CT). Furthermore, in 1 patient (Patient 10) the depth of the 9.5 Gy isodose line was more penetrating by 7 mm than the CT-based PTV depth with the clinical setup, unnecessarily overcovering the PTV at depth. This was because for the U/S-based clinical setup, without actual knowledge of the depth of the pectoralis muscle, a margin of typically 1 cm was added to the U/S determined depth of the surgical cavity to account for the U/S TV margin. Therefore, the U/S-based clinical setup overestimated the electron energy due to the added margin which projected further than the pectoralis muscle, whereas with the CT-based virtual simulation, the PTV was always trimmed such that the distal margin amounted for 2 mm from the CTV edge.

Electron energy selection was improved with CT-delineated target and virtual simulation of the electron field. Besides the advantage of good visualization of the pectoralis muscle and therefore accurate estimation of target depth offered by CT delineation, the TPS dose calculation allowed for further fine tuning of the electron energy that best covers a given target. This was achieved by sometimes using two electron energies, with appropriate weights so as to produce a more continuous spectrum of electron energies. Moreover, the selection in electron energy was highly affected by irregular patient outer surface, which was not taken into account by the clinical setup method where the chosen energy was selected to cover a certain depth in a flat, phantom-like geometry.

Target coverage and OAR sparing was superior with the CT simulation technique. Our planning aim, of PTV $V_{90\%} > 95\%$, was achieved in 100% of cases (mean $V_{90\%}$ was 98.5%) with the CT-based virtual simulation and only in 33% of the cases (mean $V_{90\%}$ was 84.4%) with the U/S-based clinical setup. Mean PTV D_{max} was 11.1 Gy with both methods, however the standard deviation was larger with the clinical setup (0.7 Gy) as compared to the CT simulation (0.2 Gy). This was because irregular patient surface was not taken into account with the

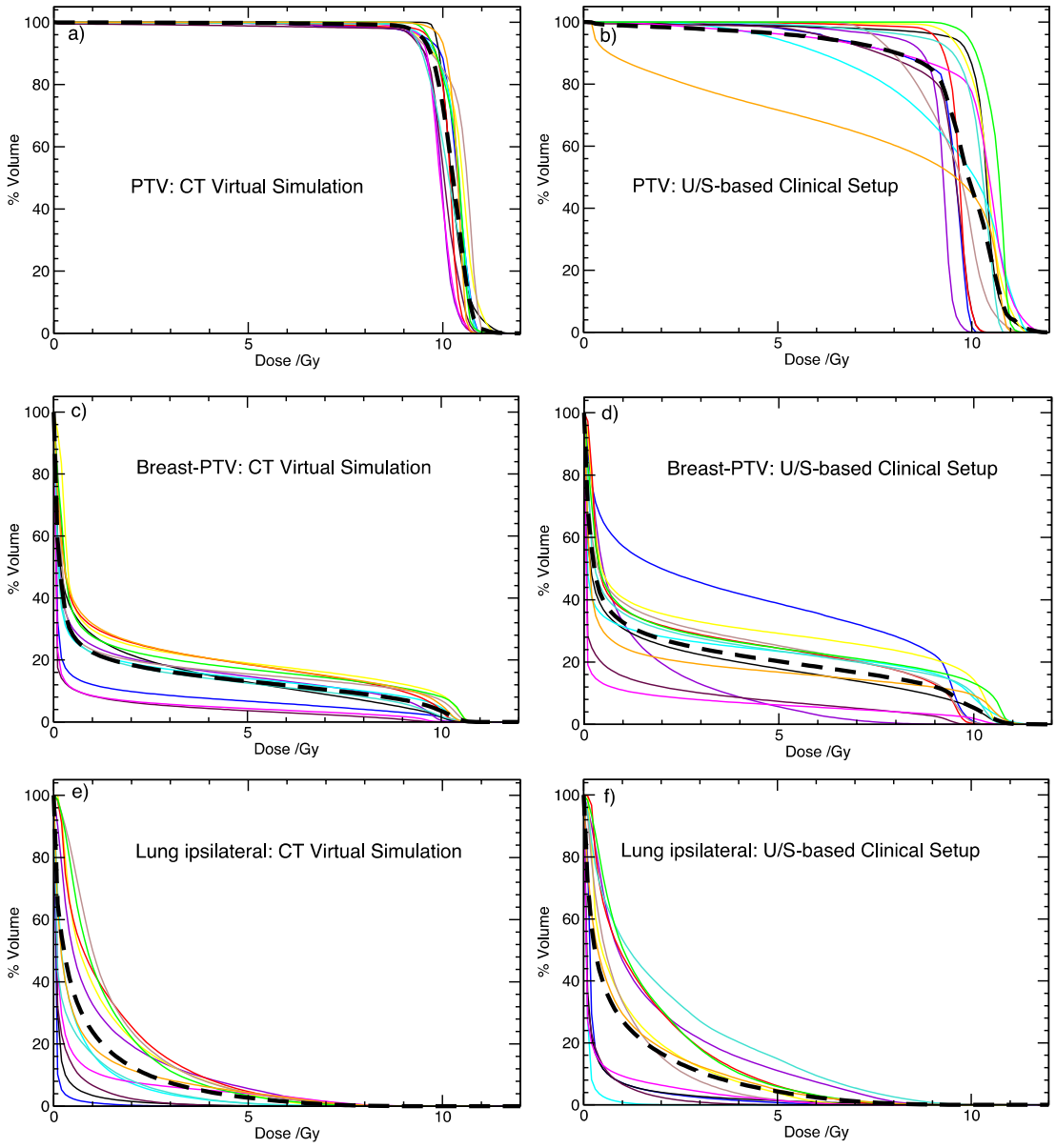

Fig. 7. PTV, breast-PTV and ipsilateral lung DVHs for CT-based virtual simulation (left-hand side) and clinical setup (right-hand side). The average DVH is shown with thick dashed line. The colour scheme used for the twelve patients is defined in Table 1.

clinical setup method.

Better normal tissue sparing for better target coverage was achieved with the CT-based virtual simulation, resulting in ipsilateral breast-PTV V_{9Gy} lower by 4.9% and V_{5Gy} lower by 7.1% ($p < 0.028$) and in ipsilateral lung V_{1Gy} lower by 3.3% ($p = 0.429$).

In the present study we used the CT target as the reference standard for our analysis. This resulted in superior target coverage with the CT-based virtual simulation since both planning and evaluation were performed on the same CT-defined target volume. For our study, the post-operative cavity was graded highly visible in one third and visible in two thirds of the cases. Ultimately, the success of the Eclipse virtual simulation hinges on the ability to accurately delineate the tumour bed on CT images. Surgical clips at the time of the lumpectomy may be used to help delineate the tumour bed. However, the use of surgical clips is not a standard practice in many centers and has not been shown to improve local control [25].

The proposed methodology for CT-based virtual simulation of the en-face electron field and collision detection between patient and electron applicator, using Eclipse TPS, has been applied in our clinic in 126 patients. Although certain details of this methodology are specific to the Eclipse TPS, the overall process can be applied on any TPS. The en-face electron field has been adequately simulated and collision was avoided in all treated cases. The overall treatment planning time CT-based virtual simulation, including electron en-face field definition, collision verification, dose calculation and plan preparation for treatment is approximately 1.5 h. Typically, the electron breast boost treatment is simulated on the planning CT scan already used for the whole breast irradiation. The clinical setup approach requires an additional patient appointment for U/S target delineation, which takes approximately 1 h. The clinical setup with patient at the treatment machine, the MU calculation and plan preparation for treatment takes approximately 45 min. The overall treatment simulation and planning time with the two techniques is similar, however the patient has two extra appointments in the radiotherapy department with the clinical setup technique.

5. Conclusions

In this study we presented a methodology for TPS virtual simulation of the electron breast boost treatments using a CT-delineated target. By addressing the issue of virtual electron simulation, all the benefits of complete 3D planning could be taken advantage of, including more accurate target delineation, better selection of electron energy and margin reduction compared to the clinical setup based on the U/S-delineated target.

Grant or financial support

None.

Meeting Presentation

None.

Declaration of Competing Interest

The authors declare that they have no known competing financial interests or personal relationships that could have appeared to influence the work reported in this paper.

Acknowledgment

None.

References

[1] Fisher B, Redmond C. Lumpectomy for breast cancer: an update of the NSABP experience. National surgical adjuvant breast and bowel project. J Natl Cancer Inst Monogr 1992:7–13.
[2] Fisher B, Anderson S, Bryant J, Margolese RG, Deutsch M, Fisher ER, et al. Twenty-year follow-up of a randomized trial comparing total mastectomy, lumpectomy, and lumpectomy plus irradiation for the treatment of invasive breast cancer. N Engl J Med 2002;347:1233–41.
[3] Clarke M, Collins R, Darby S, Davies C, Elphinstone P, Evans V, Godwin J, Gray R, Hicks C, James S, MacKinnon E, McGale P, McHugh T, Peto R, Taylor C, Wang Y, Early Breast Cancer Trialists' Collaborative Group (EBCTCG). Effects of radiotherapy and of differences in the extent of surgery for early breast cancer on local recurrence and 15-year survival: an overview of the randomised trials. Lancet 2005;366:2087–106.
[4] Romestaing P, Lehingue Y, Carrie C, Coquard R, Montbarbon X, Ardiet JM, et al. Role of a 10-Gy boost in the conservative treatment of early breast cancer: results of a randomized clinical trial in Lyon, France. J Clin Oncol 1997;15:963–8.
[5] Bartelink H, Horiot J-C, Poortmans P, Struikmans H, Van den Bogaert W, Barillot I, et al. Recurrence rates after treatment of breast cancer with standard radiotherapy with or without additional radiation. N Engl J Med 2001;345:1378–87.
[6] Graham P, Fourquet A. Placing the boost in breast-conservation radiotherapy: a review of the role indications and techniques for breast-boost radiotherapy. Clin Oncol 2006;18:210–9.
[7] Arriagada R, Mouriesse H, Sarrazin D, Clark RM, Deboer G. Radiotherapy alone in breast cancer. I. Analysis of tumor parameters, tumor dose and local control: the experience of the gustave-roussy institute and the princess margaret hospital. Int J Radiat Oncol Biol Phys 1985;11:1751–7.
[8] Denham JW. The radiation dose-response relationship for control of primary breast cancer. Radiother Oncol 1986;7:107–23.
[9] van Limbergen E, van den Bogaert W, van der Schueren E, Rijnders A. Tumor excision and radiotherapy as primary treatment of breast cancer. Analysis of patient and treatment parameters and local control. Radiother Oncol 1987;8:1–9.
[10] Landis DM, Luo W, Song J, Bellon JR, Punglia RS, Wong JS, et al. Variability among breast radiation oncologists in delineation of the postsurgical lumpectomy cavity. Int J Radiat Oncol Biol Phys 2007;67:1299–308.
[11] Ringash J, Whelan T, Elliott E, Minuk T, Sanders K, Lukka H, et al. Accuracy of ultrasound in localization of breast boost field. Radiother Oncol 2004;72:61–6.
[12] Regine WF, Ayyangar KM, Komarnicky LT, Bhandare N, Mansfield CM. Computer-CT planning of the electron boost on definitive breast irradiation. Int J Radiat Oncol Biol Phys 1991;20:121–5.
[13] Messer PM, Kirikuta IC, Bratengeier K, Flentje M. CT planning of boost irradiation in radiotherapy of breast cancer after conservative surgery. Radiother Oncol 1997;42:239–43.
[14] Machtay M, Lanciano R, Hoffman J, Hanks GE. Inaccuracies in using the lumpectomy scar for planning electron boosts in primary breast carcinoma. Int J Radiat Oncol Biol Phys 1994;30:43–8.
[15] Hepel JT, Evans SB, Hiatt JR, Price LL, DiPetrillo T, Wazer DE, et al. Planning the breast boost: comparison of three techniques and evolution of tumor bed during treatment. Int J Radiat Oncol Biol Phys 2009;74:458–63.
[16] Oh KS, Kong F-M, Griffith KA, Yanke B, Pierce LJ. Planning the breast tumor bed boost: changes in the excision cavity volume and surgical scar location after breast-conserving surgery and whole-breast irradiation. Int J Radiat Oncol Biol Phys 2006;66:680–6.
[17] Hurkmans C, Admiraal M, van der Sangen M, Dijkmans I. Significance of breast boost volume changes during radiotherapy in relation to current clinical inter-observer variations. Radiother Oncol 2009;90:60–5.
[18] Whipp EC, Halliwell M. Magnetic resonance imaging appearances in the post-operative breast: the clinical target volume-tumor and its relationship to the chest wall. Int J Radiat Oncol Biol Phys 2008;72:49–57.
[19] Goldberg H, Prosnitz RG, Olson JA, Marks LB. Definition of postlumpectomy tumor bed for radiotherapy boost field planning: CT versus surgical clips. Int J Radiat Oncol Biol Phys 2005;63:209–13.
[20] Fraser DJ, Wong P, Sultanem K, Verhaegen F. Dosimetric evolution of the breast electron boost target using 3D ultrasound imaging. Radiother Oncol 2010;96:185–91.
[21] Cygler JE, Daskalov GM, Chan GH, Ding GX. Evaluation of the first commercial Monte Carlo dose calculation engine for electron beam treatment planning. Med Phys 2004;31:142–53.
[22] Doucet R, Olivares M, DeBlois F, Podgorsak EB, Kawrakow I, Seuntjens J. Comparison of measured and Monte Carlo calculated dose distributions in inhomogeneous phantoms in clinical electron beams. Phys Med Biol 2003;48:2339–54.
[23] Smitt MC, Birdwell RL, Goffinet DR. Breast electron boost planning: comparison of CT and US. Radiology 2001;219:203–6.
[24] Aghili M, Barzegartahamtan M, Alikhassi A, Mohammadpour R. Investigation of electron boost radiotherapy in patients with breast cancer: is a direct electron field optimal? Cancer/Radiothérapie 2018;22:52–6.
[25] Fein DA, Fowble BL, Hanlon AL, Hoffman JP, Sigurdson ER, Eisenberg BL. Does the placement of surgical clips within the excision cavity influence local control for patients treated with breast-conserving surgery and irradiation? Int J Radiat Oncol Biol Phys 1996;34:1009–17.